



Supplement of

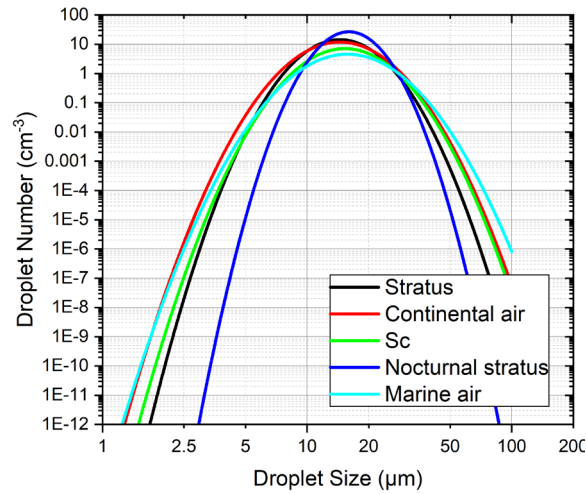
Drivers of droplet formation in east Mediterranean orographic clouds

Romanos Foskinis et al.

Correspondence to: Alexandros Papayannis (apdlidar@mail.ntua.gr) and Athanasios Nenes (athanasios.nenes@epfl.ch)

The copyright of individual parts of the supplement might differ from the article licence.

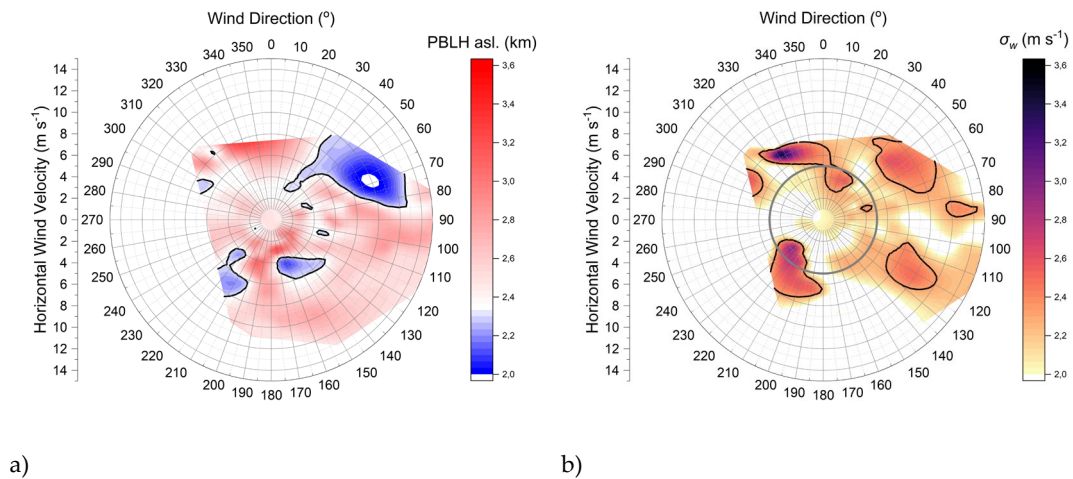
Figure S1 presents the averaged lognormal droplet size distribution for clouds with liquid water content greater than 0.1 g m^{-3} , based on Tables 1 and 2 of Miles et al. (2000) and using the grouping as defined by these authors. It is obvious that any inlet with cut-off size greater than $2.5 \mu\text{m}$ is may sample cloud droplets when in-cloud.



5 **Figure S1.** Averaged lognormal droplet size distribution for clouds with liquid water content greater than 0.1 g m^{-3} , based on Tables 1 and 2 of Miles et al. (2000).

Figures S2 (a-e) present the evolution of parameters (σ_w , eBC , N_{Total} , SO_4^{2-}) measured at (HAC)², as well as the PBLH, as a function of the horizontal wind velocity and direction. The wind speed is zero at the center of these plots and increases radially up to 14 m s^{-1} . Figure S2f presents the PDF of the wind direction for the cases when (HAC)² is within PBL (red line) or FTL (black line).

10



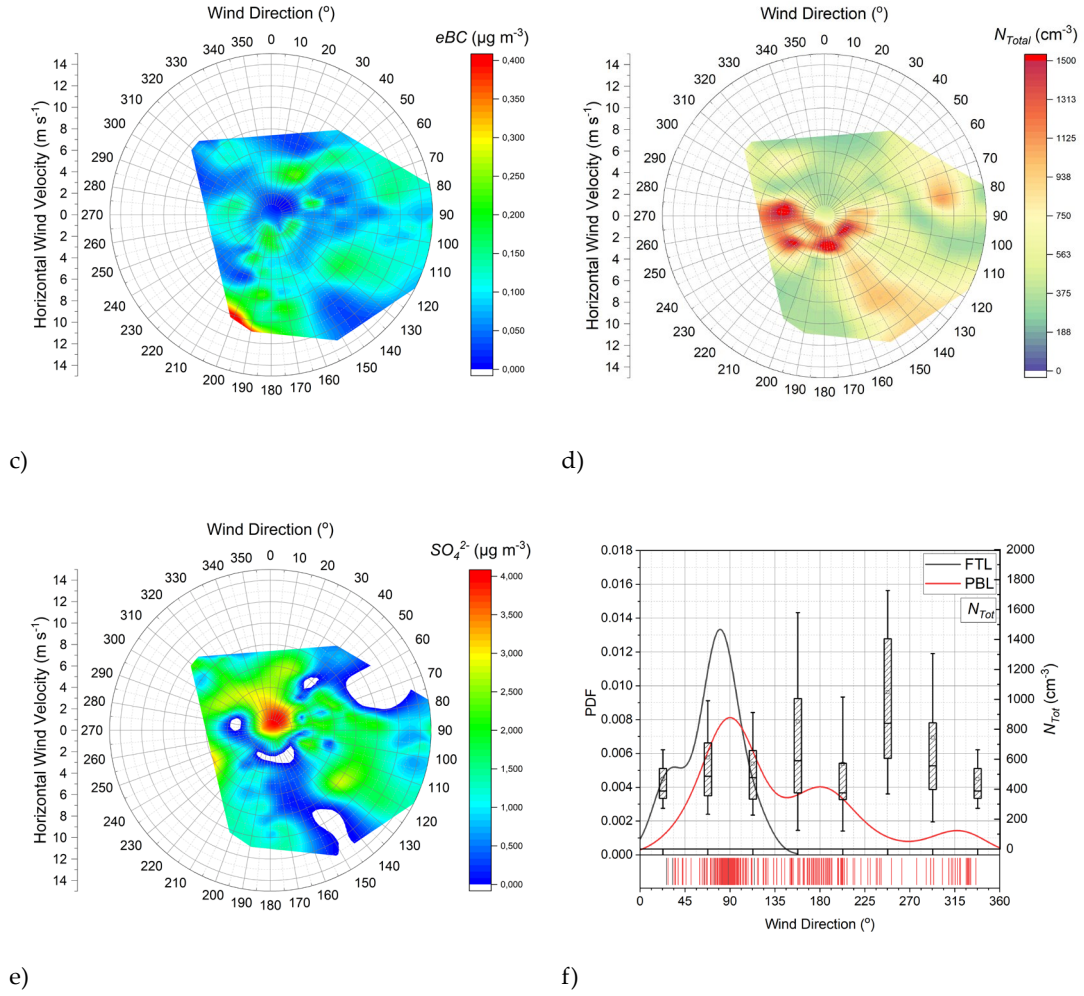


Figure S2 (a-e) Evolution of parameters (σ_w , eBC , N_{Total} , SO_4^{2-}) measured at (HAC)² during the whole measuring period, as well as the PBLH, as a function of the horizontal wind velocity and direction. f) The PDF of the wind direction for the cases when (HAC)² is within the PBL (red line) or the FTL (black line).

- 15 Figures S3 (a-c) present the statistics of N_{Total} , N_d and D_{eff} measured at (HAC)² level, when (HAC)² was within the PBL, or the FTL, under cloud-free or cloudy conditions. We found that the total number of aerosol (N_{Total}) is almost 3 times higher within the PBL, than inside the FTL (Fig. S3b). Additionally, we discuss on the aerosols effects on the droplet formation known as Twomey effect (Twomey, 1977): as shown in Figs. S3(a,b) under cloudy conditions, the increase of the aerosol content (Fig. 3b) within the
- 20 PBL leads to an increase of N_d (Fig. S3c) resulting to a decrease of the cloud droplet size (Fig. S3c), and thus, enhancing the cloud reflectance (IPCC, 2023)

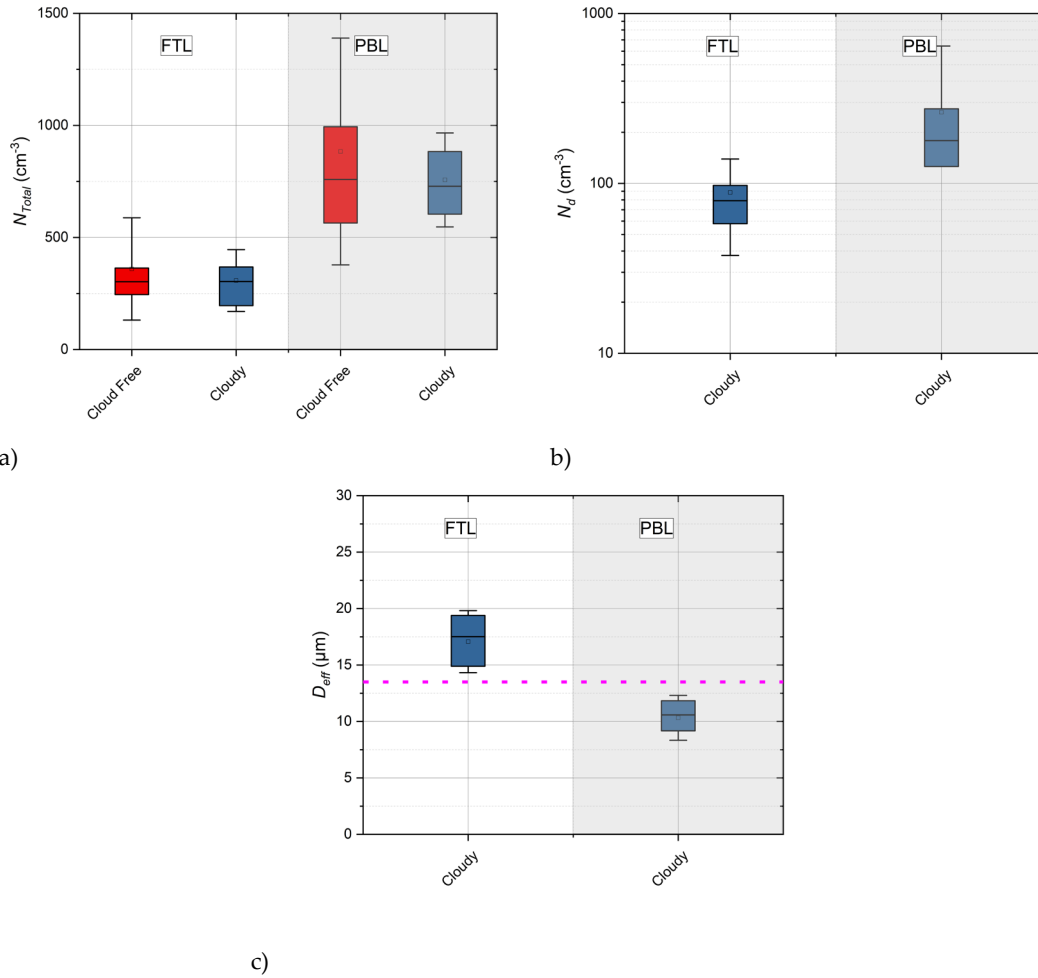
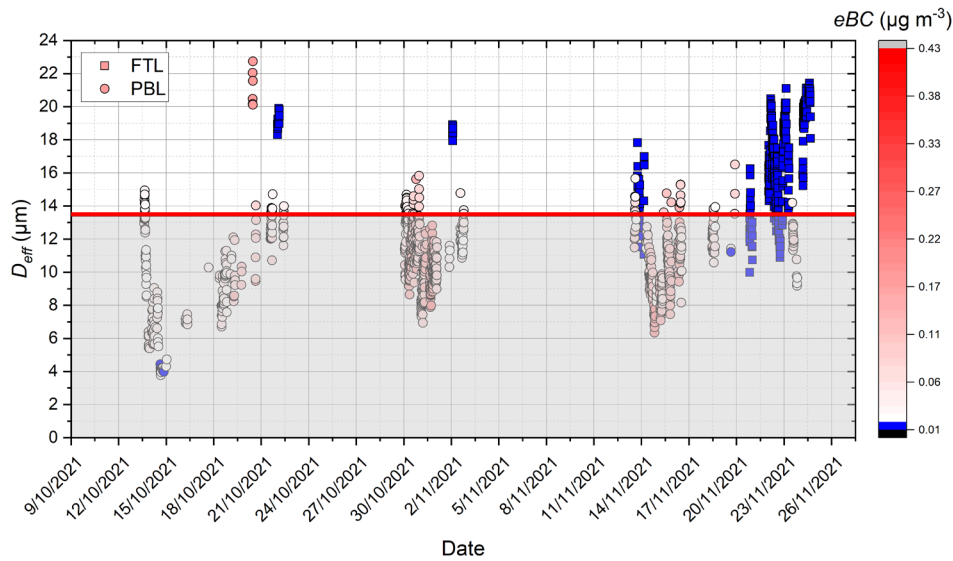


Figure S3. The boxplots of a) N_{Total} , b) N_d and c) D_{eff} measured when $(HAC)^2$ was within the PBL or under cloud-free or cloudy conditions.

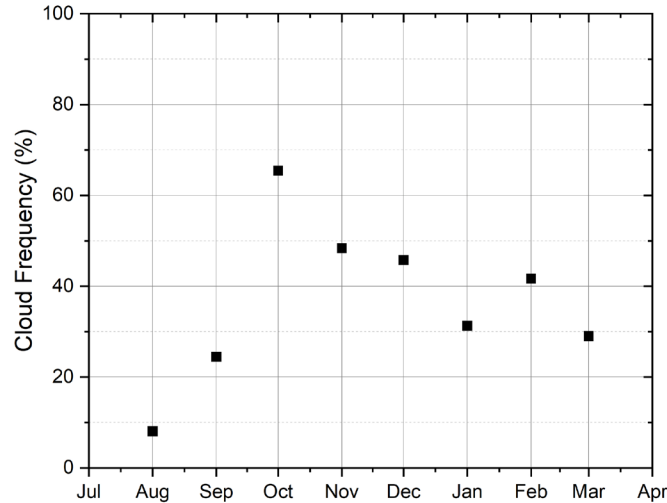
25 The time series of D_{eff} as derived by the PVM-100 are shown in Figure S4 for the cases when $(HAC)^2$ is in the PBL or the FTL. The symbol color represents the eBC concentration in $\mu\text{g}/\text{m}^3$ while the shaded area defines the cases dates) when the droplet size was smaller than the characteristic size of the inlet, and so the droplets were able to penetrate the inlet line. Low eBC concentrations (blue dots) are observed when $(HAC)^2$ is within the FTL, while high concentrations (white to red) are usually found when $(HAC)^2$ is within the PBL. Furthermore, Figure S4 also shows that clouds within the PBL tend to have more droplets

30 (Figure S3c) with smaller sizes ($D_{eff} < 13.5$ μm) (cf. Figure S3d), so the droplets with size smaller than 13.5 μm are able to penetrate into the inlet, and that is the reason why the inlet is more sensitive to PBL cloud droplets.



35 **Figure S4.** The time series of D_{eff} derived by the PVM-100 when $(HAC)^2$ is within the PBL or the FTL. The symbol color represents the eBC concentration in $\mu\text{g}/\text{m}^3$ while the shaded area defines the cases dates) when the droplet size was smaller than the characteristic size of the inlet, and so the droplets were able to penetrate the inlet line.

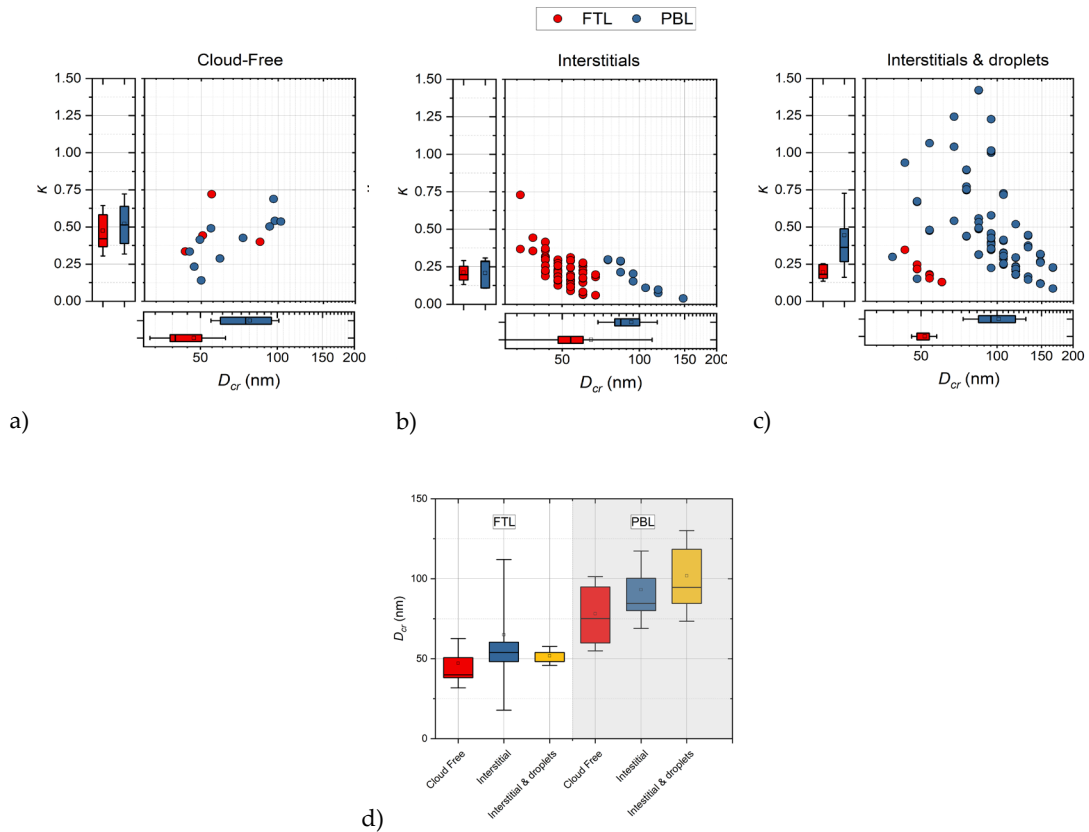
The monthly cloud coverage frequency at $(HAC)^2$ was estimated based on continues measurements of RH from August 2021 to March 2022, where as a cloud scene is considered, every moment was $\text{RH} > 95\%$. The results of the monthly cloud coverage frequency at $(HAC)^2$ are shown in Figure S5.



40 **Figure S 5.** Cloud frequency at $(HAC)^2$ based on continues measurements of RH, where as a cloud scene is considered, every moment was $\text{RH} > 95\%$.

45 The size-resolved hygroscopicity was derived for each supersaturation cycle of the CCN100, where the D_{cr} was defined at the size where the corresponding MPSS distribution, when integrated from the largest resolved size (800 nm) until the D_{cr} , gives an aerosol number equal to the observed CCN concentration. Additionally, we separated the size-resolved hygroscopicity data using the virtual-filtering technique, when $(HAC)^2$ was sampling within cloud free regimes, mixture of interstitial aerosols or only within

50 interstitial regimes (FTL or PBL) (Figure S6). What we found is that smaller particles tend to be more
 55 hygroscopic than the larger ones during cloud events – and this contrast increases when sampling a
 mixture of interstitial and dried droplets. Given that the interstitial aerosol is less hygroscopic (Figure
 S6b), the high value of hygroscopicity shown in Figure S6c, especially when the air mass originates from
 the PBL, is related to the hygroscopicity of evaporated cloud droplets. Additionally, Figure S6d reveals
 that the activated aerosols, when originating from the FTL, are smaller in size compared to particles from
 the PBL.



60 **Figure S 6.** a-c) The size-resolved hygroscopicity of the aerosols when (HAC)² was sampling within
 Cloud-Free and in-Cloud regimes, while the last was examined separately using the virtual filtering
 technique to separate the interstitial from the mixture regimes. Additionally, moments where the air mass
 was originating from FTL and PBL are indicated with red and blue marks, respectively. d) The
 distributions of D_{cr} when the air mass originating from the FTL or the PBL, respectively.